III-V/Si Tandem Cells Utilizing Interdigitated Back Contact Si Cells and Varying Terminal Configurations

Manuel Schnabel[1], Michael Rienäcker[2], Agnes Merkle[2], Talysa R. Klein[1], Nikhil Jain[1], Stephanie Essig[1*], Henning Schulte-Huxel[1], Emily Warren[1], Maikel F.A.M. van Hest[1], John Geisz[1], Jan Schmidt[2], Rolf Brendel[2], Robby Peibst[2], Paul Stradins[1], Adele Tamboli[1]

[1]National Renewable Energy Laboratory, Golden CO 80401, USA
[2]Institute for Solar Energy Research Hamelin, Emmerthal 31860, Germany
[*]now at École Polytechnique Fédérale de Lausanne (EPFL), Neuchâtel, Switzerland

***Abstract* — Integrating wide-bandgap III-V with Si solar cells has been shown to yield higher efficiencies than Si alone: As also presented at this conference, four-terminal efficiencies exceeding 32% have been attained. In this contribution, independent and electrically connected operation of the subcells in such tandem cells is examined. The optics of the tandem cell change significantly if a conducting interconnect, rather than an insulating glass slide, is required between the subcells. These effects are studied, and optically optimized structures for different types of tandem cell operation are presented. It is found that minimizing reflection at the conductive interface between the two cells while maintaining conductivity is the key challenge faced in such devices.**

I. Introduction

Solar cells made from bulk crystalline Si dominate the market, with a market share exceeding 90% [1]. However, improving efficiencies has become increasingly difficult because the current record efficiency of 26.6% [2] is already very close to the theoretical limit of 29.4% [3]. In order to achieve significantly higher efficiencies, a novel approach is required, and the one that has proven itself in practice is the tandem cell approach, with which efficiencies of 38.8% have been achieved under 1 sun illumination [4] using five junctions of III–V semiconductors. In order to substantially boost the efficiency of Si solar cells, we have been developing stacked two-junction III-V/Si tandem cells [5], recently attaining 1-sun efficiencies above 32% [6]. That said, the four-terminal (4T) operation required to achieve this efficiency may be difficult to integrate into a cost-effective module.

In this contribution, we compare the operation of an electrically connected III-V/Si tandem cell to 4T operation, from an optical viewpoint. We first present the external quantum efficiency of a 31.5% efficient (uncertified measurement) 4T GaInP/Si tandem cell, and show that all its essential features can be modeled using an in-house transfer matrix algorithm. We then apply this model to study the optics of GaInP/Si cells that are electrically connected using an EVA-based transparent conducting adhesive (TCA) [7], optimize this structure, and identify key elements required for optimized performance.

II. Experimental Details

The four-terminal tandem cell used to obtain the inputs for optical simulations was prepared from a GaInP and a Si cell. The rear heterojunction GaInP top cell [8] was grown inverted, bonded to high-index (n=1.56) glass using epoxy (also n=1.56), and then had the substrate removed. It was also processed with a front and rear side antireflective coating (MgF_2/ZnS, and ZnS, respectively, with optimized thicknesses). The Si bottom cell with doped POLy-Si on passivating Oxide (POLO) contacts was prepared using 160 µm n-type Cz-Si wafers and the process described in Ref. [9], with the cell dimensions adapted to match the top cell. The front side of the Si cell is then bonded the rear side of the glass with the GaInP on top using epoxy, aligning the cells using an infrared camera. The resulting stack is listed in Table 1.

The quantum efficiency (QE) and specular reflectance were measured on a custom-built instrument, and then used as inputs for an in-house transfer-matrix-based algorithm. This algorithm models reflection of the sample, absorption in each layer, and short-circuit current density j_{sc} if given a collection efficiency (1 for an absorber layer, 0 for all other layers unless otherwise stated). The nominal layer structure of the GaInP/Si tandem cell was fitted to the experimental QE and reflectance data, and this real layer structure modified as needed for electrically interconnected tandems. Refractive indices were obtained from in-house measurements on reference samples or from the PVLighthouse refractive index database [10-13].

III. Comparison of Simulation and Experiment for Four-Terminal Tandems

Figure 1 shows experimental external quantum efficiency (EQE) and reflection curves of a mechanically stacked 31.5% (uncertified) efficient GaInP/Si four-terminal tandem cell, prepared as described in Sec. II and Table 1. Also shown are simulated EQE and reflection curves.

The simulation begins from nominal layer thicknesses and refractive indices determined previously on reference samples. In order to fit the top cell EQE, only the top cell AlInP window layer thickness (reduced 15%), GaInP absorber layer

978-1-7281-0494-2/19/$31.00 ©2019 IEEE

thickness (reduced 5%), and GaInP absorber layer collection efficiency (reduced from 100 to 91%) are adjusted. In order to fit the bottom cell EQE, which features a front-side texture that cannot be accurately represented in a transfer matrix algorithm, the Si wafer thickness is increased (from its actual value of 150µm to 357µm) to represent the increase in optical path length that texture yields. The full layer structure modeled is given in Table 1.

Table 1: Layer stack used for simulation of four-terminal GaInP/Si tandem in Fig. 1, showing materials, thicknesses, and how much their absorption contributes to j_{sc}. Where values differ from nominal values, nominal values are given in brackets. Indispensable top and bottom cell layers are shaded blue and green, respectively, while layers present for antireflection performance are shaded grey. Optically negligible layers such as grids, or openings in layers, with small area fraction are omitted.

Material	Thickness (nm)	Contrib. to j_{sc}
air	0	0
MgF_2	97	0
ZnS	41	0
n-$Al_{0.52}In_{0.48}P$	17 (20)	0
n-$Ga_{0.5}In_{0.5}P$	950 (1000)	0.91
p-$Al_{0.27}Ga_{0.26}In_{0.47}P$	200	0
p-$Al_{0.5}Ga_{0.5}As$	500	0
ZnS	82	0
epoxy	10,000	0
glass, n=1.56	1,000,000	0
epoxy	10,000	0
PECVD SiO_x	100	0
SiN_x, n=1.91	70	0
SiN_x, n=2.4	15	0
n,p-Si	357,000 (150,000)	1
Al_2O_3	15	0
SiN_x, n=1.91	120	0
Al	10,000	0

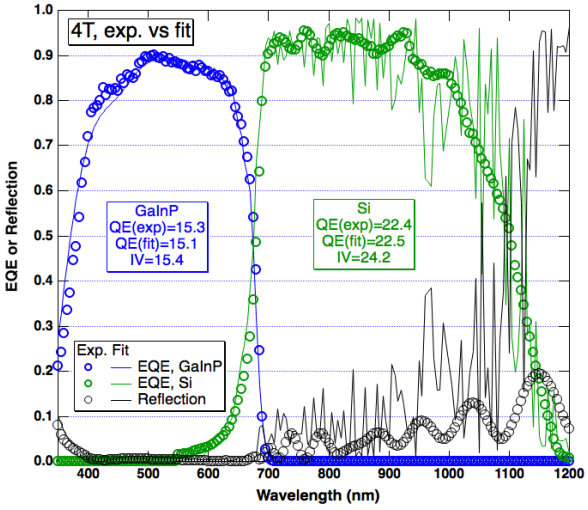

Figure 1. Experimental and simulated EQE and reflection curve for a 4T GaInP/Si tandem cell. The short-circuit currents derived from convolving the EQEs with the AM1.5G spectrum, and as measured using a solar simulator (IV), are given in the figure in mA/cm^2.

It can be seen that the external quantum efficiencies of both curves are well modeled using this approach, making only few, minor, and physically reasonable, changes to the nominal structure of the device. In particular, the imperfect charge carrier collection of 91% from the GaInP layer required for this model is feasible given an experimental internal quantum efficiency for the GaInP cell in the 85-90% range; the AlInP layer is known to vary in thickness by up to 25% based on prior growth runs, and texture is known to extend the optical path length by deflecting incident photons from normal incidence.

The main shortcomings of the model are a high-frequency oscillation at wavelengths above 700 nm, which arises from the assumption of a precisely 10 µm thick epoxy layer between the cells, whereas there is some inhomogeneity in practice; and a high reflection above ~900 nm that is not observed in experiment, which arises at least in part from the fact that only specular reflection is measured experimentally, and texture deflects much of the reflected light away from the detector (or even totally internally reflects it), whereas the model assumes flat interfaces throughout. Nevertheless, the short-circuit current densities calculated from experimental and modeled EQEs, and the overall shape of the EQE curves, are in good agreement, validating the simulation as a method to model short circuit current densities in other device structures to within ~0.3 mA/cm^2. It is not entirely clear why the j_{sc} from a solar simulator measurement matches the EQE value for GaInP cells but not for Si cells, but we will assume in the following that the deviation for Si is not wavelength dependent and that studying EQEs will permit an optimization of j_{sc}, even if the final value is an underestimation.

IV. Simulation Of Electrically Connected Tandems

The structure of an electrically interconnected tandem utilizing a TCA interconnect differs from the four-terminal structure modeled in the previous section in two key regards: only the TCA and other conductive layers can be used to optimize optics between the two cells, and the glass that is still required for mechanical stabilization of the GaInP cell must be moved to the front. These considerations, and restricting materials for antireflective layers to MgF_2 and ZnS as insulating optical layers, and thermally evaporated indium tin oxide (thermal ITO) as a conducting optical layer, leads to the initial trial structure shown in Table 2.

It consists of identical layers and layer thicknesses for the cells as Table 1, and also includes the TCA which is known to be ~50 µm thick. It does not initially include ITO layers; these will be added in further iterations as they are not strictly necessary from an electronic viewpoint: both $Al_{0.5}Ga_{0.5}As$ and Si are expected to make good contact to the TCA given sufficiently high doping. The MgF_2/ZnS double-layer antireflective coating originally present on the front of the 4T device is now separated by the front-side glass and epoxy, as both have refractive indices between those of MgF_2 and ZnS. Parameters that will be varied in the following are labeled as

such in Table 2, and simulated GaInP and Si cell j_{sc} values as a function of simulation parameters are summarized in Table 3.

Table 2: Layer stack used for simulation of electrically connected GaInP/Si tandem cells, showing materials and thicknesses (contributions to j_{sc} are assumed to be identical to those in Table 1). Initial thicknesses were carried over from Sec. III, and those that will be varied in simulations denoted as such. Indispensable top and bottom cell layers are shaded blue and green respectively, while layers present for antireflection performance are shaded grey. Optically negligible layers such as grids, or openings in layers, with small area fraction are omitted.

Material	Initial Thickness (nm)
air	0
MgF_2	97 (varied)
glass, n=1.56 (varied)	1,000,000
epoxy	10,000
ZnS	41 (varied)
n-$Al_{0.52}In_{0.48}P$	17
n-$Ga_{0.5}In_{0.5}P$	950
p-$Al_{0.27}Ga_{0.26}In_{0.47}P$	200
p-$Al_{0.5}Ga_{0.5}As$	500
ITO (varied)	0 (varied)
TCA (EVA assumed)	50,000
ITO (varied)	0 (varied)
n,p-Si	357,000
Al_2O_3	15
SiN_x, n=1.91	120
Al	10,000

Simulating the structure in Table 2 and comparing results to Fig. 1 shows that while the top cell j_{sc} only decreases 0.2 mA/cm^2, the bottom cell j_{sc} takes a large hit in this new and unoptimized cell architecture, decreasing by 6.2 mA/cm^2 (first two rows of Table 3). Optimizing the MgF_2 and ZnS thicknesses reveals that the initial thicknesses (97 nm, 41 nm) were already close to optimal (97 nm, 47 nm) for maximizing current in the current-limiting GaInP cell (Table 3, "Optimizing for Limiting Current"), as would be desired in a two-terminal tandem cell. Changing the glass used from high-index glass (n=1.56) matched to epoxy to commercial borosilicate glass (n=1.52) leads to an optimized GaInP j_{sc} that is only 0.1 mA/cm^2 lower, indicating that the type of glass used is not critical in initial stages of device optimization, provided the MgF_2 and ZnS thicknesses are readjusted. It also has a negligible effect on the Si cell's j_{sc}. For series-connected cells therefore, the initial structure in Table 2 is largely sufficient, and while the coupling of light into both cells might be improved using textured instead of planar front glass, the much poorer coupling of light into the bottom cell is still sufficient for the Si cell not to limit current.

Turning now to electrically connected devices that extract the full power of each cell, such as 3T devices, a need for further adaptation of the tandem structure in order to lower the 6.2 mA/cm^2 j_{sc} loss of the Si cell is apparent. Examining the simulation of the initial structure in Table 2, and of the structures optimized for current-matched performance, reveals that the mean reflection for wavelengths above 700 nm is ~35% (not shown). There are two conceivable reasons for this: either the front of the tandem structure in Table 2 (MgF_2/glass/epoxy/ZnS) only exhibits antireflective performance below 700 nm, or the interface between the GaInP and Si cell, which only light above ~700 nm reaches, is particularly reflective. Taking the structure in Table 2 and setting the TCA (EVA) thickness to zero while keeping all other parameters constant raises the j_{sc} of the Si cell from 16.3 mA/cm^2 to 23.3 mA/cm^2, higher than in an optimized four-terminal device. This indicates that the TCA is responsible for the high reflectivity above 700 nm, which must be mitigated.

Table 3: Simulated short-circuit current densities in the GaInP and Si cells of an electrically connected tandem connected using an EVA-based TCA and having front-side glass. Values for a four-terminal device from Fig. 1 are also shown for comparison. The second block of data is for current-matched operation, while the third block is for maximum power output from each cell.

Variation	GaInP j_{sc} (mA/cm^2)	Si j_{sc} (mA/cm^2)
Four-Terminal (Table 1)	15.1	22.5
Initial Interconnected (Table 2)	14.9	16.3
Optimizing for Limiting Current		
n=1.56 glass	15.0	16.4
borosilicate glass	14.9	16.4
Optimizing for Maximum Power		
2x thermal ITO	14.8	19.8
2x 1.7E19 sputtered ITO	14.7 (14.4)[a]	23.3 (23.6)[a]
2x 1E20 sputtered ITO	14.7	22.8
2x 6E20 sputtered ITO	14.8	17.4
1x thermal ITO	14.8	18.6

[a]PVLighthouse raytracing [14] result of same stack.

The high reflectivity upon introducing the TCA is not surprising: its main component, EVA, has a mean refractive index of 1.49 between 600 and 1200 nm, as compared to 3.4 for $Al_{0.5}Ga_{0.5}As$ and 3.7 for Si, yielding two highly reflective interfaces. This reflection can be reduced by introducing a conductive, transparent layer with intermediate refractive index such as ITO at these two interfaces. These two ITO layers are added to the simulation, and thicknesses of both ITO layers, and of front-side MgF_2 and ZnS, varied iteratively to reach an optimum output. Since the optimization is to be for maximum power extraction, and GaInP cells have roughly twice the maximum power point voltage of Si cells, the expression $(2j_{sc,GaInP}+j_{sc,Si})$ is optimized. Adding 84 nm thermal ITO above and below the TCA, together with optimized MgF_2 and ZnS thicknesses yields 14.8 mA/cm^2 in the GaInP cell and 19.8 mA/cm^2 in the Si cell, thus recovering more than half the j_{sc} loss observed in the Si cell upon switching from the structure in Table 1 to that in Table 2, while enduring only marginal reductions in j_{sc} of the GaInP cell.

Nevertheless, there is still room for improvement, as 23.3 mA/cm^2 were modeled for the Si cell when the reflective TCA layer is absent. We now consider the nature of the ITO,

as inputs used were for in-house thermal ITO, which is known to have non-ideal transparency. The aforementioned simulation is repeated for sputtered ITO with carrier concentrations of 0.17, 1, and 6×10^{20} cm^{-3}, whose complex refractive indices are taken from Ref. [10]. The results are shown in Table 3; for the three sputtered ITOs trialed, a Si cell j_{sc} of 23.3, 22.8, and 17.4 mA/cm^2, respectively, was obtained, with GaInP j_{sc} being equal within the error of the simulation. The stack with the lowest-doped ITO was also simulated with the raytracer from PVLighthouse [14] to account for texture on the Si cell, yielding a GaInP cell j_{sc} of 14.4 mA/cm^2 and a Si cell j_{sc} of 23.6 mA/cm^2 and lending additional credibility to the transfer matrix modeling. It is thus shown that an electrically interconnected GaInP/Si tandem can harvest as much light as an optimized four-terminal device; however, insertion of an ITO layer (or other transparent conductor) with adequate refractive index and extinction coefficient is crucial.

In practice, while lower-doped ITO is better optically, it may not contact the TCA as well, leading to a trade-off between fill factor and j_{sc} in actual cell optimization. In addition, little is known about the electrical properties of the proposed p-$Al_{0.5}Ga_{0.5}As$/ITO junction; III-V semiconductors are rarely combined with transparent conducting oxides as transparent conductors can be realized within the III-V group of compounds, and ITO is a n-type material. For this reason, we perform one last optimization, in which the ITO between p-$Al_{0.5}Ga_{0.5}As$ and TCA is omitted, but retained between TCA and Si. Comparing the two "thermal ITO" rows of Table 3, it can be seen that incorporating only this one thermal ITO layer hardly affects the j_{sc} of the GaInP cell but decreases j_{sc} of the Si cell by 1.2 mA/cm^2. We expect that this effect may be tolerable if p-$Al_{0.5}Ga_{0.5}As$/ITO junctions are poor. More generally, the transparent conductors inserted between either cell and the TCA are absolutely critical in achieving good performance, both from an electrical and optical viewpoint.

V. Conclusions

The external quantum efficiencies, and hence short-circuit current densities, of GaInP/Si tandem solar cells stacked for four-terminal or electrically connected operation have been studied. The former was used to validate the optical model by demonstrating a good fit to experimental data. The latter was used to study the optical interlayers required when the two cells have glass on top, instead of between the cells, and are connected by a TCA of relatively low refractive index.

It was shown that a current density only 0.2-0.3 mA/cm^2 lower is readily attained in the current-limiting GaInP cell in the electrically connected structure. The Si cell exhibits higher current than the GaInP cell in all scenarios investigated, indicating that if current-matched operation is desired, no interlayers are required between the cells and the TCA from an optical viewpoint. This is however not optimal in terms of extracting maximum power from a GaInP/Si tandem cell, and if the electrically connected tandem is to be operated in a manner that allows the full power of each subcell to be collected, e.g. in a 3T device, the strong reflection at the interfaces between the TCA and the two cells must be suppressed. This can be successfully achieved by introducing ITO layers at these two interfaces, but only if the ITO is sufficiently transparent and has the correct refractive index. Engineering of transparent conducting interlayers such as ITO at these two interfaces is expected to be key to realizing effective light management and carrier transport in GaInP/Si tandem cells that are electrically connected with a TCA.

Acknowledgments

Funding for this work at NREL was provided by DOE through EERE contract SETP DE-EE00030299 and under Contract No. DE- AC36-08GO28308. Funding at ISFH was provided by the EU's FP7 under grant # 608498, as well as by the German Federal Ministry for Economic Affairs and Energy under grant # FKZ0324040. The United States Government retains and the publisher, by accepting the article for publication, acknowledges that the United States Government retains a non-exclusive, paid-up, irrevocable, world- wide license to publish or reproduce the published form of this manuscript, or allow others to do so, for United States Government purposes.

The ISFH authors wish to thank Thomas Friedrich, Frank Heinemeyer, Jan Hensen, Sabine Kirstein, Heike Kohlenberg, Tobias Neubert, Annika Raugewitz, David Sylla, Marta Tatarzyn and Nadine Wehmeier from ISFH for the processing solar cells. A special thank is due to Guido Glowatzki, Jan Krügener and Bernd Koch from the Institute of Electronic Materials and Devices of Leibniz University Hanover for helping with polysilicon deposition and ion implantation and the Laboratory of Nano and Quantum Engineering (LNQE) of Leibniz University of Hanover for support.

References

[1] Fraunhofer-ISE, "Photovoltaics Report," 17.11.2016 2016.

[2] NREL, "NREL Efficiency Chart," ed. This plot is courtesy of the National Renewable Energy Laboratory, Golden, CO., 2017.

[3] A. Richter, M. Hermle, and S. W. Glunz, "Reassessment of the limiting efficiency for crystalline silicon solar cells," *IEEE Journal of Photovoltaics,* vol. 3, pp. 1184-91, 2013.

[4] M. A. Green, K. Emery, Y. Hishikawa*, et al.*, "Solar cell efficiency tables (version 49)," *Progress in Photovoltaics: Research and Applications,* vol. 25, pp. 3-13, 2017.

[5] J. V. Gee, Gary, "A 31%-Efficient GaAs/Silicon mechanically-stacked, multijunction concentrator solar cell," *IEEE Electron Device Letters,* pp. 754-758, 1988.

[6] S. Essig, C. Allebe, T. Remo*, et al.*, "32% efficient III-V/Si dual-junction solar cells and their challenging path towards cost competiveness " *submitted to 44th IEEE PVSC,* 2017.

[7] T.R. Klein, M. Schnabel, E.L. Warren*, et al.*, "Transparent Conductive Adhesives for Tandem Solar Cells," *Proceedings of the 44th IEEE PVSC,* 2017.

[8] J. F. Geisz, M. A. Steiner, I. García, *et al.*, "Enhanced external radiative efficiency for 20.8% efficient single-junction GaInP solar cells," *Applied Physics Letters,* vol. 103, p. 041118, 2013.
[9] M. Rienaecker, M. Bossmeyer, A. Merkle, *et al.*, "Junction Resistivity of Carrier-Selective Polysilicon on Oxide Junctions and Its Impact on Solar Cell Performance," *IEEE Journal of Photovoltaics,* vol. 7, pp. 11-18, 2016.
[10] Z. C. Holman, M. Filipič, A. Descoeudres, *et al.*, "Infrared light management in high-efficiency silicon heterojunction and rear-passivated solar cells," *Journal of Applied Physics,* vol. 113, p. 013107, 2013.
[11] P. Kumar, M. K. Wiedmann, C. H. Winter, *et al.*, "Optical properties of Al2O3 thin films grown by atomic layer deposition," *Applied Optics,* vol. 48, pp. 5407-5412, 2009/10/01 2009.
[12] M. Vogt, "Development of physical models for the simulation of optical properties of solar cell modules," Ph.D., Faculty for Mathematics and Physics, Leibniz Universität Hannover, 2015.
[13] K. R. McIntosh, T. C. Kho, K. C. Fong, *et al.*, "Quantifying the optical losses in back-contact solar cells," in *2014 IEEE 40th Photovoltaic Specialist Conference (PVSC)*, 2014, pp. 0115-0123.
[14] (9. June 2017). *PV Lighthouse: Module Ray Tracer*. Available: https://http://www.pvlighthouse.com.au